J. Phys.: Condens. Matter **8** (1996) 5235–5245. Printed in the UK

Physical properties of the giant magnetoresistive perovskite system La–Er–Ca–Mn–O

D Bahadur†§, M Yewondwossen†, Z Koziol†, M Foldeaki‡ and R A Dunlap†

† Department of Physics, Dalhousie University, Halifax, Nova Scotia, Canada B3H 3J5

‡ Institut de Recherche sur l'Hydrogène, Université du Québec à Trois-Rivières, Trois-Rivières, Québec, Canada G9A 5H7

Received 27 February 1996, in final form 19 April 1996

Abstract. The effect of minor changes in lattice parameters and Mn^{3+}/Mn^{4+} ratios on the magnetoresistive and related properties of the La–Er–Ca–Mn–O perovskite system have been investigated. The latter is found to be the more important factor in determining the magnetotransport properties of these materials. One composition has been prepared by both the standard ceramic method as well as a sol–gel technique. Although the general features of the magnetotransport properties of these two samples were very similar, the magnetic properties showed significant differences. Experimental results are explained on the basis of a spin-dependent mechanism which is related to lattice distortion.

1. Introduction

Rare-earth–manganese-oxide-based perovskites have attracted considerable attention recently as a result of their giant magnetoresistance (GMR) behaviour near the ferromagnetic ordering temperature [1–3]. Most of the early work in this field was on epitaxial thin films of $Ln_{1-x}M_xMnO_3$ (Ln = rare-earth ion; M = Ca, Ba, Sr) with variations in compositions, substrate and growth procedures [4–6]. Early attempts to observe this interesting phenomenon in polycrystalline samples were unsuccessful and this has been attributed to causes such as grain boundary effects [4, 5]. However, there are now several reports of the observation of GMR effects in polycrystalline samples [7–11]. From some of these studies [8, 10] and on the basis of early reports [12], it appears that the GMR effects are strongly influenced by the substitution at the A site of the ABO_3 perovskite structure of ions of different ionic radii. While making substitutions for the A-site atoms, it is important that the Mn^{3+}/Mn^{4+} ratio should be maintained at around 7/3, which is ideal for the existence of ferromagnetic interactions and metallic behaviour resulting from the double-exchange mechanism [8]. In addition to substitution by divalent ions, such as Ca^{2+}, this ratio is also very sensitive to the oxygen stoichiometry [11]. The critical parameters appear to be (a) the average ionic radius of the A-site atoms, (b) the Mn^{3+}/Mn^{4+} ratio and (c) the tolerance factor, which is given by [8]

$$t = \frac{R_A + R_O}{\sqrt{2}(R_B + R_O)} \tag{1}$$

§ On leave from: Department of Metallurgical Engineering and Materials Science, Indian Institute of Technology, Powai, Bombay 400 076, India.

0953-8984/96/285235+11$19.50

where R_i is the ionic radius of the A, B or O ions. There has recently been a report of a large magnetoresistance effect at 140 K in a La–Y–Ca–Mn–O perovskite system by Jin *et al* [7]. Similar or larger effects have also been recently reported in the Sm–Sr–Mn–O [13] and Pr–Sr–Ca–Mn–O systems [10]. All the systems so far reported to exhibit GMR effects in polycrystalline samples have values of the three parameters given above which fall within certain critical limits. It appears that by carefully monitoring and controlling these parameters, it could be possible to design materials with optimized magnetoresistive properties and transition temperature. Among the first few reports on the polycrystalline samples, the work by Jin *et al* on the composition $La_{0.6}Y_{0.07}Ca_{0.33}MnO_3$ has yielded some interesting results [7]. Following along similar lines we have, in the present work, investigated similar compositions where Y has been replaced by the rare earth erbium. The ionic radius of erbium comes closest to that of yttrium among the lanthanide series and hence the composition $La_{0.6}Er_{0.07}Ca_{0.33}MnO_3$ should, in principle, behave similarly if lattice effects (i.e. ionic radii at the A site) are the only important criteria. However, if electronic structure and/or chemical properties of the A-site ions are also important we would expect Er- and Y-containing compounds to show different properties. We have also varied the method of preparation for this composition to see whether the properties are sensitive to the method of synthesis. In addition, we have synthesized the following two compositions: $La_{0.57}Er_{0.1}Ca_{0.33}MnO_3$ and $La_{0.57}Er_{0.13}Ca_{0.3}MnO_3$, by ceramic methods. We have varied the erbium content by a small amount (0.03%) so that the average ionic radii at the A site and the tolerance factor change slightly. We have also varied the calcium content by a small amount to investigate the effect of the Mn^{3+}/Mn^{4+} ratio. All of the ceramic samples have been synthesized under identical conditions to ensure that the oxygen stoichiometry does not change from sample to sample. The samples have been characterized by x-ray diffraction to monitor the formation of the single-phase perovskite structure. Following this the magnetization and magnetoresistance studies were carried out and the salient features of the results are discussed in this paper.

2. Experimental methods

For the ceramic samples, the required amount of either oxides or carbonates of the different constituent elements were mixed and the mixture was heated very slowly up to 1225 K and held at that temperature for a period of six hours. The decomposed powder was again mixed and was pelletized, and the pellet was heated to 1725 K for six hours in air and then cooled slowly to room temperature. For the citrate gel method, the required amount of rare-earth oxides, calcium oxide and manganese metal were slowly dissolved in nitric acid and the solution was evaporated to dryness. The residue was then dissolved in distilled water and the required amount of citric acid diammonium salt solution in water was added under controlled pH conditions. The solution was then refluxed for about 12 hours. The sol thus obtained was slowly evaporated to obtain the gel. The gel was subsequently dried and heated slowly to about 875 K for the citrate complex to decompose. The fine powder thus obtained was then processed further as for the ceramic samples.

The x-ray diffraction patterns were recorded with a Siemens D-500 scanning diffractometer using Cu Kα radiation. The electrical resistivity and magnetoresistivity were measured as a function of temperature between 4.2 K and 300 K and in an applied magnetic field up to 6 T. Temperature-dependent magnetization measurements were performed between 4.2 and 330 K using a conventional dc SQUID magnetometer in an applied field of 1 T. Magnetization versus field measurements were performed for fields up to 7 T and between temperatures of 10 and 200 K.

Table 1. Details of the perovskite samples studied in this work; lattice parameter, a, of the elementary perovskite cell; average ionic radius at the A site, R_A; tolerance factor, t; and resistivity, ρ, at 5 K and 300 K. g in parentheses indicates that the sample was made by the citrate gel process, all other samples have been made by the ceramic route.

Sample	Composition	a (Å)	R_A (Å)	t	$\rho_{5\,K}$ (Ω cm)	$\rho_{300\,K}$ (Ω cm)
1	$La_{0.6}Er_{0.07}Ca_{0.33}MnO_3$(g)	3.858	1.136	0.9399	0.045	0.13
2	$La_{0.6}Er_{0.07}Ca_{0.33}MnO_3$	3.850	1.136	0.9399	0.024	0.09
3	$La_{0.57}Er_{0.1}Ca_{0.33}MnO_3$	3.858	1.129	0.9382	0.02	0.11
4	$La_{0.57}Er_{0.13}Ca_{0.30}MnO_3$	3.862	1.126	0.934	1.39	0.13

3. Results and discussion

The x-ray diffraction patterns of all the samples showed them to be of the single-phase cubic perovskite structure. No evidence of any secondary phase was seen in any of the samples. Table 1 gives the lattice parameter, the average ionic radius of the A-site ions, the tolerance factor and resistivity values at 5 K and room temperature.

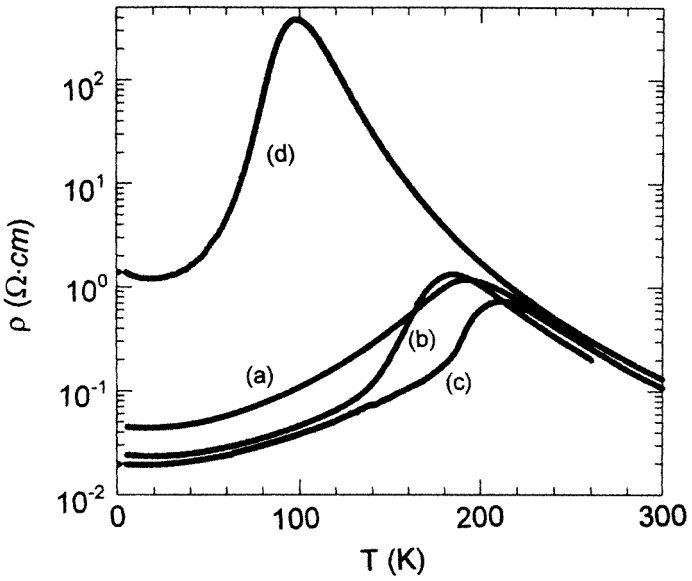

Figure 1. Zero-field resistivity as a function of temperature for the samples identified in table 1; (a) sample 1, (b) sample 2, (c) sample 3 and (d) sample 4.

Figure 1 shows the zero-field resistivity as a function of temperature for the samples currently investigated. All of the samples exhibit a maximum near the Curie transition. Above the transition semiconductor-like behaviour with negative $d\rho/dT$ is observed, while below the transition, metallic-like behaviour with positive $d\rho/dT$ is seen. It is noteworthy that the behaviour of all of the samples above the transition temperature (e.g above the maxima) is essentially identical indicating that the mechanism for transport is similar in all of the samples in this temperature regime. There are, however, obvious variations below

this temperature where the samples are magnetically ordered. Another important feature of the zero-field resistivity data is the minima observed at low temperature, around 40 K. This is most prominent for sample 4 and has been reported for other GMR materials by other researchers (see, e.g., [14]). While samples 1, 2 and 3 have transitions at similar temperatures, sample 4 shows the transition at much lower temperature. Also, the change in the resistivity at the transition temperature is much larger for sample 4 compared to the other samples studied here.

A comparison of the results from samples 1 and 2 is informative for understanding the effects of sample preparation technique on the resulting sample property. A comparison of the results from samples 2, 3 and 4 allows for an assessment of the influence of composition. In these samples, either the calcium content or the oxygen stoichiometry would decide the ratio of Mn^{3+} to Mn^{4+}. It is assumed that the oxygen stoichiometry is the same for all ceramic samples as they have been synthesized under identical conditions. It is well known that the metallic and ferromagnetic behaviour result from double-exchange interactions between Mn^{3+} and Mn^{4+} ions in these oxides. Therefore, this ratio is critical in determining properties such as the Curie temperature. From the zero-field resistivity data as shown in figure 1, it appears that the Mn^{3+}/Mn^{4+} ratio is more influential than the other parameters tested here in determining sample properties. Most of the features as discussed above are different for sample 4 where the Mn^{3+}/Mn^{4+} ratio has been changed by a small amount.

The temperature dependence of magnetization for all of the samples measured in an applied field of 1 T is illustrated in figure 2. The values of the Curie temperature as indicated by the magnetization measurements are in general agreement with the location of the peak in the resistivity measurements. A comparison of the magnetization values at 5 K for the different samples shows some noteworthy differences. For example, there is a large difference between magnetization values of samples 1 ($\sim$20 emu g^{-1}) and 2 ($\sim$100 emu g^{-1}). Also, for these two samples their temperature dependences of spontaneous magnetization are quite different, although their zero-field resistivities (see figure 1) are similar in many respects. As mentioned above, both of these samples are of the single-phase cubic perovskite structure. However, their lattice constants are different. X-ray measurements as shown in table 1 give a larger lattice parameter for the sample synthesized by the citrate gel method (sample 1) compared with the sample prepared by ceramic methods (sample 2). Since the compositions of the samples 1 and 2 are same, it is likely that these differences are the result of variations in the oxygen stoichiometry. Oxygen deficiency in sample 1 could result in a larger concentration of Mn^{3+}, which has larger ionic radii than Mn^{4+}. Ju *et al* [11] have investigated $La_{0.67}Ba_{0.33}MnO_z$ where they have varied the oxygen stoichiometry between 2.99 and 2.80 and have observed a similar effect. They have also observed reduced magnetization values and a broader Curie transition for oxygen-deficient samples. This is similar to what is seen here for the sample made by the citrate gel process. It is not entirely clear, however, why the sample synthesized through the citrate gel process becomes more oxygen deficient although it is reasonable to assume that a substantial quantity of oxygen is used to form oxides of carbon and nitrogen during the decomposition of the citrate–nitrate complex. It is also of relevance to point out the anomalous behaviour of the magnetization of sample 1 in the region of about 50 K. This behaviour is reproducible, and although the reasons for this anomaly are not yet clearly known, similar anomalies have been reported by other authors [15] and have been attributed to a possible antiferromagnetic transition. The difference in the magnetization versus temperature behaviour for samples 1 and 2 can be ascribed to competing ferromagnetic and antiferromagnetic interactions which are sensitive to Mn–Mn or Mn–O–Mn distances. There are indications of corresponding

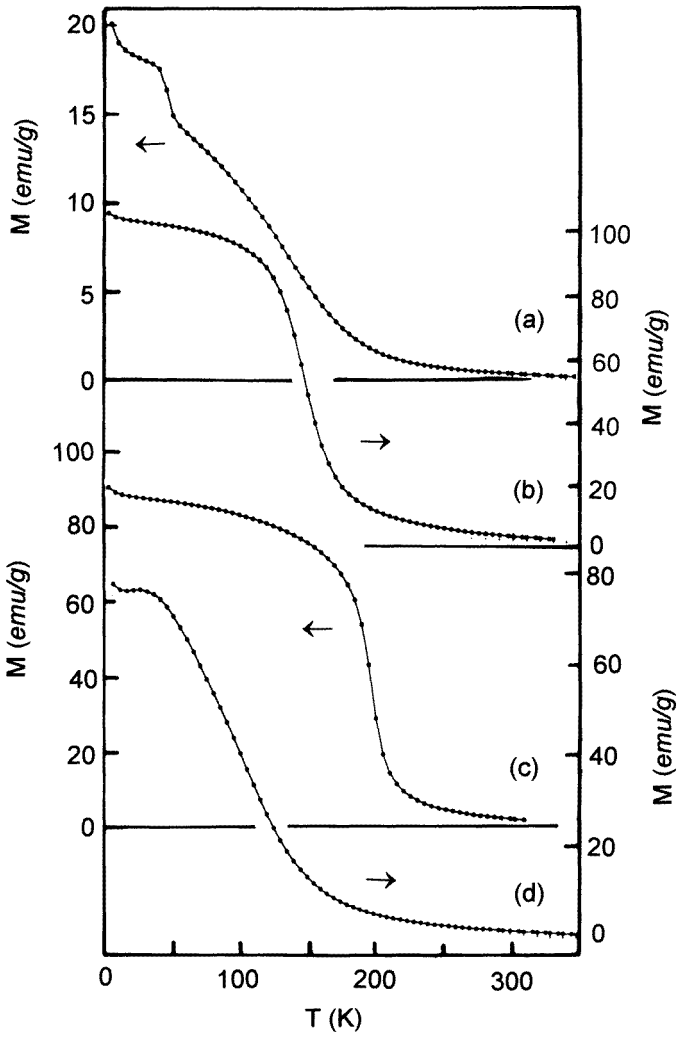

Figure 2. Temperature-dependent magnetization measured in an applied field of 1 T for (a) sample 1, (b) sample 2, (c) sample 3 and (d) sample 4.

variations in the lattice parameters of these two samples.

A typical plot of magnetization versus magnetic field at different temperatures for sample 2 is shown in figure 3. The magnetization shows a sharp increase as a function of field up to about 0.5 T, although it does not show complete saturation even in applied fields of up to 7 T. This type of behaviour is typical of systems with canted spins. The competition between double-exchange ferromagnetism (FM) and exchange antiferromagnetism may result in canted antiferromagnetism in these materials [11, 16].

To gain more insight into the behaviour of these materials, the resistivity has been measured as a function of applied magnetic field and is illustrated in figure 4 for two of the samples. It is interesting to note that this plot shows two distinct regions corresponding to the two distinct regions in the magnetization versus field behaviour. Up to about 0.5 T

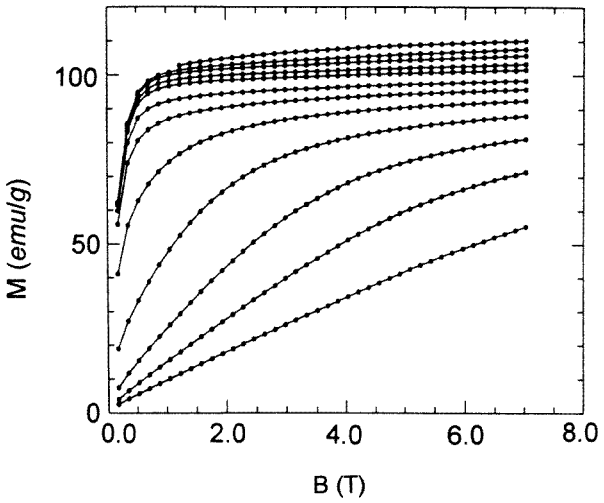

Figure 3. Magnetization as a function of applied field for the sample $La_{0.60}Er_{0.07}Ca_{0.33}MnO_3$ (sample 2) at different temperatures. Decreasing values of the magnetization correspond to the temperatures 10, 25, 40, 65, 80, 105, 120, 135, 150, 165, 180 and 200 K.

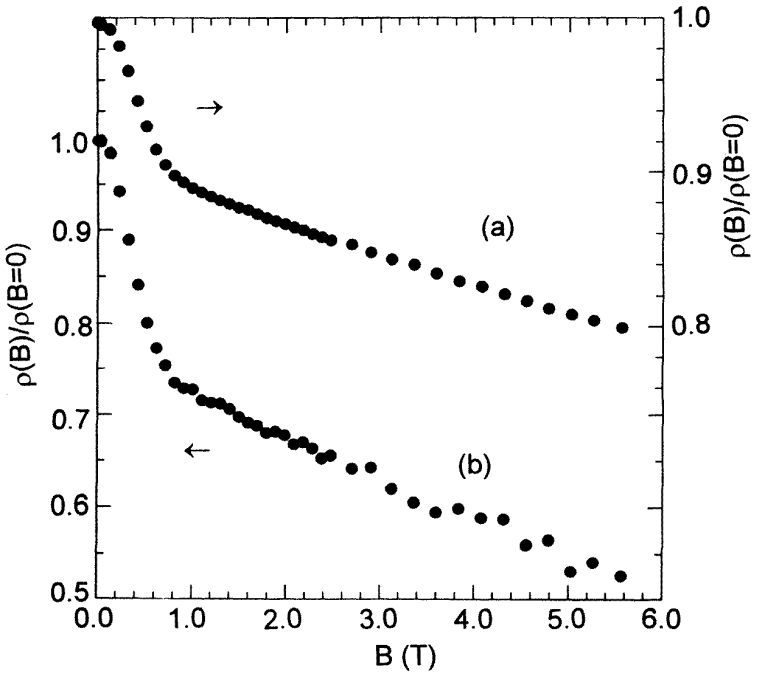

Figure 4. Normalized resistivity as a function of applied magnetic field at 5 K for (a) sample 1 and (b) sample 2.

the magnetoresistance drops sharply, and above this field value, the slope is much smaller. These effects seem to be related to the movement and rotation of the domain walls consisting

of Mn^{3+} and Mn^{4+} spins coupled through the double-exchange mechanism. Such concepts were explored earlier [11, 17, 18]. We suggest the following plausible explanation based on the movement and rotation of the domain walls. When the applied field is low, there are a large number of domains and hence a large density of domain walls. Within the domain walls, spins are not parallel but change direction slowly with respect to adjacent domains so as to minimize the sum of the exchange and anisotropy energies. In these regions, electron transfer between Mn^{3+} and Mn^{4+} does not occur as readily as it does within the domain wall itself. This results in a higher resistivity in the low-field region where the domain wall density is large. As the applied field is increased, the number of domain walls is reduced significantly resulting in a rapid drop in resistivity. The field where the slope of the magnetoresistance changes corresponds to the near-saturation field in the magnetization curves. Here the sample consists primarily of a single domain, and subsequent changes in magnetization occur principally as a result of domain rotation and changes in the spin canting angle within the domain. This results in much smaller changes in the magnetoresistance as seen in figure 4.

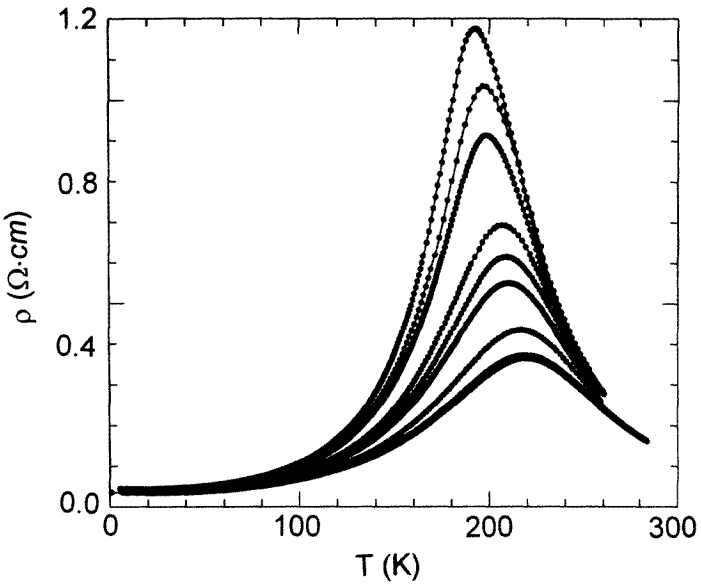

Figure 5. Resistivity as a function of temperature for different field values for sample 1. Decreasing values of the peak resistivity correspond to the field values of 0, 0.5, 1.0, 2.0, 2.5, 3.0, 4.0 and 5.0 T.

The resistivity data in fields up to 5 T as a function of temperature for the different samples are illustrated in figures 5 to 8. The magnetoresistance ratios, $\Delta\rho/\rho_0$, may be estimated as

$$\frac{\Delta\rho}{\rho_0} = \frac{\rho_B - \rho_0}{\rho_0} \tag{2}$$

where the ρ_0 is the zero-field electrical resistivity and ρ_B is the resistivity in the maximum applied field. This ratio varies between 73 and 98% for the present samples. The maximum change is observed for sample 4; about 98% in an applied field of 5 T. This is comparable to that reported by Jin *et al* [7] for $La_{0.6}Y_{0.07}Ca_{0.33}MnO_3$ where a maximum change of

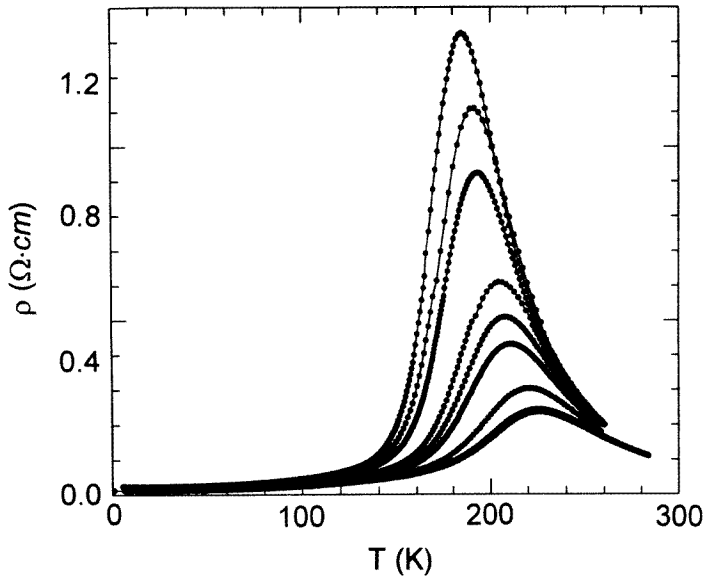

Figure 6. Resistivity as a function of temperature for different field values for sample 2. Decreasing values of the peak resistivity correspond to the field values of 0, 0.5, 1.0, 2.0, 2.5, 3.0, 4.0 and 5.0 T.

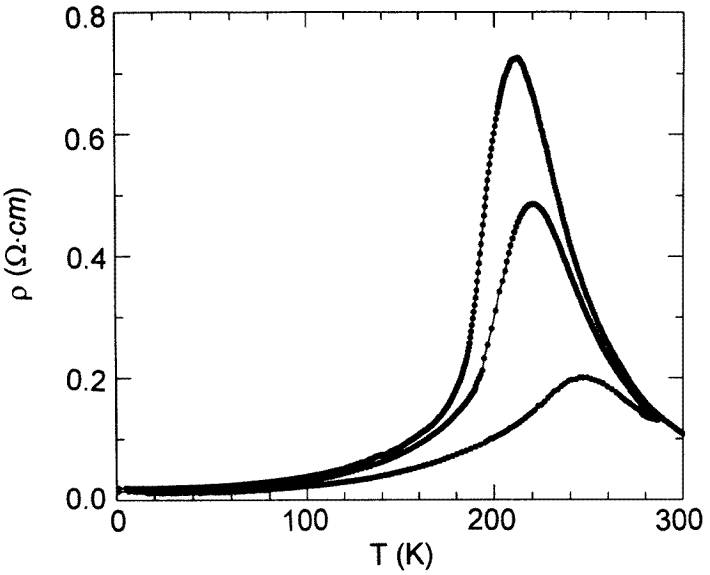

Figure 7. Resistivity as a function of temperature for different field values for sample 3. Decreasing values of the peak resistivity correspond to the field values of 0, 1.0 and 4.0 T.

99% in an applied field of 5 T was observed. This corresponds to a change of 10 000% according to their definition of the magnetoresistance ratio. These plots exhibit a shift in the maxima to higher temperatures as the field increases. This feature has been reported

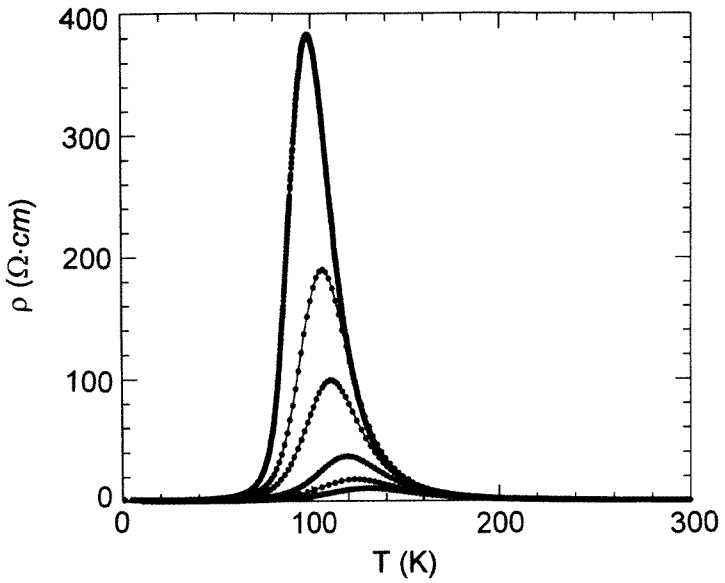

Figure 8. Resistivity as a function of temperature for different field values for sample 4. Decreasing values of the peak resistivity correspond to the field values of 0, 0.5, 1.0, 2.0, 3.0 and 4.0 T.

for several other systems [14, 19] and appears to be characteristic of materials exhibiting giant magnetoresistance effects. The fact that the transition is field dependent and lies close to the ferromagnetic transition temperature indicates that the spin-dependent mechanism is responsible for these effects. This spin-dependent mechanism which results from the Mn^{3+}–O^{2-}–Mn^{4+} interaction is a strong function of the distortion of the lattice, if the Mn^{3+}/Mn^{4+} ratio remains constant. This is also reflected in the studies by Hwang *et al* [8] and Jia *et al* [14], where they have introduced lattice distortion by the substitution of smaller ions at the A sites. Interestingly this affects the transition temperature and the change in the magnitude of the resistivity in much the same way as the application of a magnetic field. An important parameter for the measurement of lattice distortion in this family of perovskites is the tolerance factor as defined by equation (1). For $t \approx 1$ a cubic structure results giving a Mn–O–Mn bond angle, θ, close to 180°. However, the factor t is generally less than 1, resulting in a deviation of this angle from 180°. Experimental evidence shows that the Curie temperature is proportional to the angle θ [8, 20]. In $RNiO_3$-type compounds (R = rare earth), Torrance *et al* [20] have shown that as the tolerance factor and/or temperature increases, the bandwidth increases and the compounds become more metallic. The magnetic ordering temperature also simultaneously increases and this is accompanied by slight reduction in unit-cell volume. These authors have shown that as the average rare-earth-ion size at the A site decreases (the tolerance factor decreases), the ABO_3 structure becomes more distorted and the BO_6 octahedra tilt and rotate in order to fill the space otherwise present around the rare-earth ion giving a lower B–O–B angle. A substantial effect of temperature on the B–O–B angle has also been by reported by Torrance *et al* [20]. Other reports have also emphasized the importance of the interpolated cation and the tolerance factor in relation to the GMR effect in these manganites [10, 13]. The applied magnetic field is known to bring about a change in the canting angle or even induce a

structural phase transition in these manganites [3]. Both the B–O–B bond angle and the spin canting angle could be responsible for the spin-dependent mechanism. Hence, compositional variations and applied magnetic fields may have similar effects on the resistivity.

As indicated above, the zero-field resistivity above the transition temperature is essentially identical for all of the present samples. An analysis of the data in this region is helpful in understanding the details of the transport mechanisms in these materials. Previous reports have suggested the application of the variable-range-hopping model, which is based on the formation of magnetic polarons [14, 21], to the zero-field resistivity data above the Curie temperature. Magnetic polarons, in the form of conduction electrons, polarize the magnetic moments of the surrounding ions to form small ferromagnetic regions. These magnetic polarons can become localized and conduction then occurs through the variable-range-hopping process. Previous analysis has suggested that the applicability of this model to these GMR materials is demonstrated by a linear relationship between $\ln(R/R_{4.2})$ and $T^{-1/4}$. We have undertaken a non-linear least-squares analysis of the present data to a more general function of the form

$$\rho(T) = A \exp\left[\frac{B}{T^n}\right] \tag{3}$$

where A, B and n are free fitting parameters. The most reliable results may be obtained for sample 4 because of its much lower Curie temperature. The limited amount of data above the transition temperature for the other samples reduced the reliability of the analysis for these cases. Over a range of temperatures from 120 K to 300 K the resistivity of sample 4 yields the following fitting parameters: $A = 1.05 \times 10^{-16}$ Ω cm, $B = 115.2$ K^n and $n = 0.23$. In general the parameter n is related to the dimensionality of the system, d, by $n = 1/(d+1)$. The present value of n near 1/4 illustrates the applicability of this model and suggests that a dimensionality of 3 is appropriate for the conduction mechanisms in these materials.

4. Conclusions

We have investigated the magnetoresistance and related properties for erbium-substituted La–Ca–Mn–O-based perovskites. Changes in the calcium content of the compound seem to influence the properties more than changes in the erbium content. This behaviour may be related to changes in Mn–O–Mn bond angle and Mn^{3+}/Mn^{4+} ratio. The method of synthesis does not substantially affect the magnetoresistance properties, although it has significant effects on the magnetization of the material. This may be explained by the influence of spin-dependent mechanisms and is consistent with the general conclusion that the magnetic properties are more sensitive to the microstructural details than are the transport properties. The magnetoresistance in the paramagnetic region can be satisfactorily modelled on the basis of the variable-range-hopping model for a material with a dimensionality of 3.

References

[1] Jonker G H and van Santen J H 1950 *Physica* **16** 337
[2] von Hemlolt R, Wecker J, Holzapfel B, Schultz L and Samwer K 1993 *Phys. Rev. Lett.* **71** 2331
[3] Asamitsu A, Moritomo Y, Tomioka Y, Arima T and Tokura Y 1995 *Nature* **373** 407
[4] Jin S, Tiefel T H, McCormack M, Fastnacht R A, Ramesh R and Chen L H 1994 *Science* **264** 413
[5] Jin S, McCormack M and Tiefel T H 1994 *J. Appl. Phys.* **76** 6929
[6] Chahara K, Ohno T, Kasai M and Kozono Y 1993 *Appl. Phys. Lett.* **63** 1990
[7] Jin S, O'Bryan H M, Tiefel T H, McCormack M and Rhodes W W 1995 *Appl. Phys. Lett.* **66** 382

[8] Hwang H Y, Cheong S W, Radaelli P G, Marezio M and Batlogg B 1995 *Phys. Rev. Lett.* **75** 914
[9] Mahesh R, Mahendiran R, Raychaudhuri A K and Rao C N R 1995 *J. Solid State Chem.* **114** 297
[10] Raveau B, Maignan A and Caignaert V 1995 *J. Solid State Chem.* **117** 424
[11] Ju H L, Gopalakrishnan J, Peng J L, Li Q, Xiong G C, Venkatesan T and Greene R L 1995 *Phys. Rev.* B **51** 6143
[12] Goodenough J B and Longo J M 1970 *Landolt–Börnstein Tabellen* vol III/4a (Berlin: Springer)
[13] Caignaert V, Maignan A and Raveau B 1995 *Solid State Commun.* **95** 357
[14] Jia Y X, Lu L, Khazeni K, Yen D, Lee C S and Zettl A 1995 *Solid State Commun.* **94** 917
[15] Radaelli P G, Cox D E, Marezio M, Cheong S W, Schiffer P E and Ramirei A P 1995 *Phys. Rev. Lett.* **75** 4488
[16] Yoshizawa H, Kawano H, Tomioka Y and Tokura Y 1995 *Phys. Rev.* B **52** 13 147
[17] von Hemlolt R, Wecker J, Lorenz T and Samwer K 1995 *Appl. Phys. Lett.* **67** 2093
[18] Xiong G C, Li Q, Ju H L, Baghat S M, Lofland S E, Greene R L and van Katesan T 1995 *Appl. Phys. Lett.* **67** 3031
[19] De Teresa J M, Blasco J, Ibarra M R, Garcia J, Marquina C, Algarabel P and del Moral A 1995 *Solid State Commun.* **96** 627
[20] Torrance J B, Lacorre P, Nazzal A I, Ansaldo E J and Niedermayer C 1992 *Phys. Rev.* B **45** 8209
[21] Coey J M D, Viret M, Ranno L and Ounadjela K 1995 *Phys. Rev. Lett.* **75** 3910